



# Wastewater treatment at the Houghton Lake wetland: Temperatures and the energy balance

Robert H. Kadlec

Wetland Management Services, 6995 Westbourne Drive, Chelsea, MI 48118-9527, USA

## ARTICLE INFO

### Article history:

Received 23 October 2008

Received in revised form 10 January 2009

Accepted 9 March 2009

### Keywords:

Treatment wetlands  
Water temperature  
Soil temperature  
Energy  
Cycles

## ABSTRACT

This paper describes the temperatures in surface water and soils in a very long-running study of the capacity of a natural peatland to remove nutrients from treated wastewater. Two zones were found, an adaptation zone near the discharge to the wetland, and a background zone comprised of areas more than about 100 m from the discharge. The discharge zone was transformed to a floating mat during the 30-year course of the project. Strong diurnal cycles in surface water temperatures were measured, with a median daily swing of about 6–10 °C. Pumped water was a few degrees warmer than the wetland background, and was reduced in temperature by passage through the adaptation zone. The time constants for adaptation (63% of change) were approximately one-half to 1 day. Soil temperatures followed a cyclic pattern, with decreasing amplitude with depth, and a time delay increasing with depth. The seasonal surface maximum was about 18 °C. The irrigation season started on May 1, with water at 10 °C, and ended in early October, with water at 10 °C. The soil conduction model was used to infer cyclic surface temperatures, with a smoothed result compared to synoptic temperature measurements in surface water. Background zone fitting parameters were the Julian day of surface maximum temperature (196), mean temperature (7.9 °C), surface amplitude (10.3 °C), and penetration depth (1.0 m). Soil heat fluxes were vertically downward during the warm season, and back up toward the surface with maxima of 1.4 MJ/m<sup>2</sup> d in the discharge zone. This vertical soil heat flux was of small importance to the summer energy budget, which was dominated by solar radiation and evaporative cooling.

© 2009 Elsevier B.V. All rights reserved.

## 1. Introduction

The performance of the community of Houghton Lake (Lat. 44° 19'N, Lon 84° 46'W) treatment wetland has been continuously monitored over a 30-year period of operational record (POR), spanning 1978–2007. Details of the project history and other aspects of the project have been described in Kadlec (2009a,b,c). The features of the project that are important to the energy budget and temperatures are summarized here. The climate is north temperate. The wetland is characterized by dense cattails. Wastewater from the Houghton Lake community is treated in two aerated lagoons, and stored in a third pond during the cold half of the year. This treated water is transferred during the summer half-year to a smaller pond, and thence to an existing peatland located about 2 km from the ponds. This treated water enters a 700 ha wetland, and is further treated to background water quality in an irrigation area of approximately 100 ha. A central portion of about 30 ha developed into a floating cattail mat, with under-mat flow.

Prior to wastewater irrigation, about 10–30 cm standing water was usually present in spring and autumn, but the wetland had no surface water during dry summers. Irrigation created a 100% hydroperiod in the irrigation area. Soils were 1–2 m of highly decomposed sedge peat in most locations, with 2–5 m of medium-decomposition sphagnum peat in other zones.

Water was distributed along a 1 km gated pipeline located interior to the wetland (see system layouts in Kadlec, 2009a,b,c). Wastewater added to the interior surface sheet flow. This overland flow proceeded from northeast down a 0.02% gradient to a stream outlet and beaver dam seepage. The annual seasonal flows from the community to the wetland increased from 400,000 to 700,000 m<sup>3</sup> over the POR, and were typically introduced during about 120 days during the allowable 182-day operations period. This operational window was set based upon the average times of freeze-up and the spring thaw. The temperature of the pumped water ranged from 10 to 25 °C, with a midsummer maximum.

The physical and chemical environment of a wetland affects all biological processes, which are major determinants of treatment potential. Two of the most widely fluctuating and important abiotic factors are soil and water temperature (*T*). In turn, temperature is an important modifier of other abiotic variables, including dissolved

E-mail address: [rhkadlec@chartermi.net](mailto:rhkadlec@chartermi.net).

oxygen (DO) and hydrogen ion concentration (pH). Temperature responses of rates of respiratory CO<sub>2</sub> emission from plants–soil ecosystems are frequently modeled using exponential functions with a constant  $Q_{10}$  of approximately 3.0 (fractional change in rate with a 10 °C increase in temperature). For instance, Boone et al. (1998) report  $2.3 < Q_{10} < 4.6$  for CO<sub>2</sub> emission under a variety of soil conditions. As a consequence, the annual cycle in soil temperature produces cyclic responses in CO<sub>2</sub> production. Furthermore, the generation and emission of other greenhouse gases, such as methane and nitrogen oxides, respond to soil temperature levels and cycles (Zhang et al., 2002). Soil temperature has been found to have strong effects on the species composition, stem density and biomass of wetland plants (Seabloom et al., 1998).

Because temperature exerts a strong influence on chemical and biological processes, it is important to wetland design. This is especially true for nitrogen processing, for which the rates are strongly temperature dependent. Nitrification and denitrification are known to change by factors of three or more over the water  $T$  range of 0–20 °C.

## 2. Methods

Onset Optic Stowaway™ submersible temperature loggers were deployed on May 25, 1997, in the cattail area at the discharge and a sedge control area about 700 m from the discharge. (See Kadlec, 2009a for a pictorial representation.) These loggers were preset to record and store temperature every hour over the course of the irrigation season. They were retrieved (on October 26, 1997), after recording 3720 values. In each area, one logger was placed at the bottom of the water column, in the litter layer, and a second logger was placed in the soil below (30 cm below soil surface in the discharge area, and 45 cm below in the sedge control area). The loggers were individually cross-calibrated to a mercury thermometer. During the following irrigation season, temperature loggers were deployed on May 25, 1998, along a gradient from the cattail discharge to the sedge control area. These loggers were preset to record and store temperature every hour over the course of the irrigation season. They were retrieved (on October 14, 1998), after recording 3475 values. In each area, the logger was placed at the bottom of the water column, in the litter layer.

At various times during the POR, surface water temperatures were measured with hand-held thermocouple probes and indicating meters. On five occasions during each irrigation season 1998–2002, a Hanna™ K-thermocouple microcomputer thermometer, with a 2-m long temperature probe, was used to determine vertical soil temperature profiles at several distances from the discharge, on approximately monthly frequency during the unfrozen seasons. Measurements were taken at five or six depths in the peat layer, spaced 30 cm apart. During 1978–1979, soil temperature measurements were taken at the 30 cm vertical spacing, at various distances from the discharge, but additionally at closer vertical intervals on some occasions. Locations were identified by the distance from the discharge in meters, followed by the letter “C” designating a central transect line.

Daily minimum and maximum air temperatures were available from the National Oceanographic and Atmospheric Administration Houghton Lake 6WSW meteorological station located 6 km away.

## 3. Calculations

The quantitative representation of the spatial and temporal trends to be expected in wetland water and soil temperatures has been described in various sources (Kadlec and Wallace, 2008). A brief summary is presented here.

### 3.1. Annual cycles

Wetland water temperature varies seasonally, as do air temperatures (Kadlec, 1999). Data for water temperatures from the irrigation discharge area and control areas were regressed to a truncated, sinusoidal time series model of the form:

$$T = T_{\text{avg}}(1 + A \cos[\omega(t - t_{\text{max}})]) \quad (1)$$

where  $A$  = fractional half amplitude of the annual temperature, °C;  $t$  = time, Julian day;  $t_{\text{max}}$  = time of annual maximum temperature, Julian day;  $T$  = water temperature, °C;  $T_{\text{avg}}$  = annual average unfrozen water temperature, °C;  $\omega$  = annual frequency,  $\omega = 2\pi/365 = 0.0172 \text{ year}^{-1}$ .

This formulation has been proven to provide an excellent fit to wetland water temperatures during the unfrozen season (see for example Kadlec, 2006). The raw data from the loggers were averaged over a 24-h period to generate the mean daily water and soil temperatures. Daily air temperatures were then smoothed using a cosine function Eq. (1), to avoid the confusion of data scatter.

### 3.2. Adaptation trends

A treatment wetland typically contains two thermal regions. There is an inlet region in which water temperatures adjust to the prevailing meteorological conditions, and an outlet region in which that adjustment is complete (Kadlec and Wallace, 2008). After adjustment, temperature does not change further with distance, or detention time. This is the balance temperature, which changes seasonally. For short detention times (typically less than 3–5 days), the adjustment may not be completed, and the balance temperature is not reached (Kadlec, 2006).

A spatially distributed energy budget, in the direction of flow, can provide a good representation of temperature variation with distance or detention time; but it is difficult to implement, because of the requirement for extensive meteorological data. An empirical exponential model provides an adequate representation, and may be easily calibrated:

$$\begin{aligned} T &= T_b + (T_i - T_b) \cdot \exp(-\eta t / \rho c h) \\ T &= T_b + (T_i - T_b) \cdot \exp(-t / \tau_A) \end{aligned} \quad (2)$$

where  $h$  = water depth, m;  $T$  = wetland water temperature, °C;  $T_b$  = wetland balance temperature, °C;  $T_i$  = inlet water temperature, °C;  $\eta$  = accommodation coefficient, MJ/m<sup>2</sup> d °C;  $\rho c$  = volumetric heat capacity of water, MJ/m<sup>3</sup> °C;  $t$  = nominal detention time, d;  $\tau_A$  = accommodation time, d.

The quantity  $\tau_A = \rho c h / \eta$  represents characteristic thermal accommodation time for the wetland, during which 63.2% of the change from inlet to outlet (balance) temperature has been achieved. At  $3\tau_A$ , 95.0% of the change has been accomplished. However, for many other wetlands and conditions, there may be no adaptation region, and hence no plateau. The balance  $T$  may exist everywhere. For instance, water may enter at the balance temperature.

### 3.3. Soil temperatures

Vertical energy transport in wetland soils has been modeled as transient heat conduction, and fits data quite well for other wetlands (Priban et al., 1992; Mihalakakou et al., 1997; Kadlec, 2001; Kadlec and Wallace, 2008). The temperature profiles  $T(z,t)$  in the soils below a wetland are governed by the unsteady state heat conduction equation together with the boundary condition of a fixed

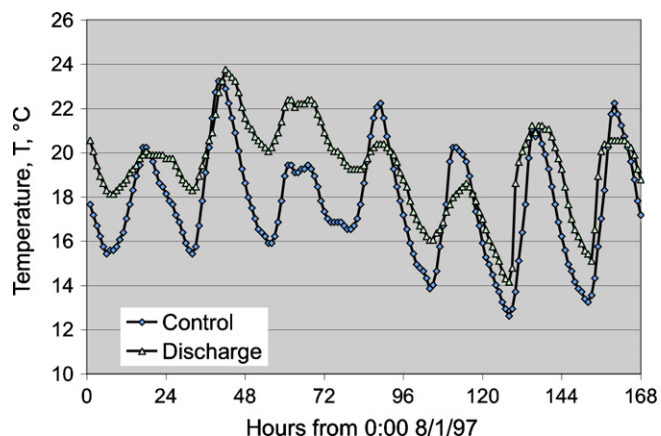


Fig. 1. Hourly water temperatures in the control and discharge zone, 1997. These temperatures were measured in the surface water, at the top of the litter layer.

mean annual temperature, a constant at deep locations:

$$\frac{T^2}{z^2} = \frac{1}{\alpha} \frac{T}{t} \quad (3)$$

$$T(\infty, t) = T_s \quad (4)$$

For a sinusoidal surface temperature, the solution to this periodic, dynamic heat balance is (Priban et al., 1992):

$$T(z, t) = T_s + A \exp\left(-\frac{z}{H}\right) \cos\left[\omega(t - t_{\max}) - \frac{z}{H}\right] \quad (5)$$

where

$$H = \sqrt{\frac{2\alpha}{\omega}} \quad (6)$$

and

$$\alpha = \frac{k}{\rho_s c_s} \quad (7)$$

and where  $A$  = amplitude of surface temperature cycle, °C;  $c_s$  = soil heat capacity, MJ/kg °C;  $k$  = soil thermal conductivity, MJ/m d °C;  $t$  = time, Julian day;  $t_{\max}$  = time of maximum surface temperature, Julian day;  $T$  = temperature, °C;  $T_s$  = mean annual temperature of the soil surface, °C;  $z$  = vertical depth, m;  $\alpha$  = thermal diffusivity of soil, m<sup>2</sup>/d;  $\rho_s$  = soil density, kg/m<sup>3</sup>;  $\omega$  = annual cycle frequency =  $2\pi/365 = 0.0172 \text{ d}^{-1}$ .

The penetration depth ( $H$ ) is the depth at which the mean annual temperature swing is 63.2% of that at the soil surface ( $A$ ). The heat flux ( $G$ ) into (or out of) the water from the soil is then:

$$G = \left[\frac{kA}{H}\right] \cdot \{\cos[\omega(t - t_{\max})] - \sin[\omega(t - t_{\max})]\} \quad (8)$$

It may be shown that the heat flux ( $G$ ) achieves a maximum 46 days (one-eighth of an annual cycle) before the day of minimum water temperature, which is also 136 days after the day of maximum water temperature. It may also be shown that the total heat gain from the soil over the 182-day heating half cycle ( $G_{\text{half}}$ ) is:

$$G_{\text{half}} = (2\sqrt{2}) \frac{kA}{\omega H} \quad (9)$$

#### 4. Water temperature cycles

Air and wetland water temperatures are subjected to both diurnal and annual cycles, corresponding to the cycles in solar radiation (Kadlec, 1999). The swing in wetland water temperature from day to night was considerable in control and discharge areas (Fig. 1). The differences between the daily maxima and minima, over the

Table 1

Diurnal swings in water temperatures, averaged over the irrigation season (mean  $\pm$  sd). Raw data were hourly values at the top of the litter layer and in the soil layer. The control site (700C) was dry a good share of the irrigation season in 1998. Data in 1984 represent measurements on four dates, June–August.

	Maximum (°C)	Minimum (°C)	Swing (°C)
Air			
1997	21.1	5.9	15.2
Water			
1984			
Discharge (0C)	28.0	11.3	16.8
Control (700C)	29.5	11.8	17.8
1997			
Discharge (0C)	18.0	14.9	3.1 $\pm$ 1.3
Control (700C)	17.5	12.7	4.8 $\pm$ 2.1
1998			
Discharge (0C)	20.8	14.0	6.7 $\pm$ 3.3
220C	20.3	12.5	7.9 $\pm$ 3.2
500C	21.3	11.0	10.4 $\pm$ 4.5
Control (700C)	29.9	8.7	20.0 $\pm$ 10.0
Soil			
1997			
Discharge (30 cm)	18.6	17.5	1.11 $\pm$ 0.79
Control (45 cm)	11.8	11.6	0.14 $\pm$ 0.12

irrigation season, are shown in Table 1. The diurnal swing in water temperatures had a mean of 6.5 °C in the water, but only about 0.6 °C in the soils. Both were typically less than the diurnal swing in air temperature. The minimum in water temperature was typically at 8:00 AM, and the maximum at 5:00 PM. Therefore, the entire swing was experienced during the course of a normal working day.

The diurnal variations in the temperatures were large in the control area when it was dry, and nearly absent in the discharge zone at the same time. The amplitude of the diurnal cycle was about 18 °C for the control area, with the maximum occurring about 4:00 PM for the third week in June, 1998. In contrast, the diurnal swing was only 2–3 °C in the discharge zone.

The annual cycles in water temperature closely resembled the annual cycles in mean daily air temperature, with maxima in mid-July. Those cycles for water are truncated in autumn, by the advent of freeze-up, and resume again in spring, with the spring thaw. The cyclic parameters for air and pumped and surface waters in 1997 are given in Table 2. It should be noted that annual cycle means are not the same as seasonal means, because of the half-year irrigation season.

The various fits to probe data showed the seasonal maximum occurred on July 14 (Julian day  $196 \pm 6$ ). That maximum water temperature along the transect through background sites was  $18.2 \pm 0.6$  °C. That was cooler than the pumped water, which averaged 19.9 °C for the season.

The loggers indicated only small differences in seasonal average water temperatures at discharge and background locations during 1997–1998. Discharge sites averaged  $17.0 \pm 4.9$  °C, and background sites averaged  $16.0 \pm 4.0$  °C. Based upon transect data, any site more than 100 m from the discharge was considered a background site, because there were no trends in temperatures for distances greater than 100 m (see following section). The cyclic trend maximum temperatures were 18.4 °C at the 700C control site (2.4 °C above the seasonal mean), and 21.1 °C at the discharge site (4.1 °C above the seasonal mean). Thus the surface water temperatures were a few degrees warmer at the discharge locations, likely reflecting the warmer pumped water. The full seasonal time trend of daily air and water temperatures is shown in Fig. 2.

**Table 2**  
Parameters of the annual cyclic sinusoidal fit to air and water temperatures for 1997.

	Mean (°C)	Amplitude (°C)	Annual peak yearday	Variability of departures sd (°C)	R <sup>2</sup>	Data frequency
Air						
Max	10.1	17.47	206	4.77	0.96	Daily
Mean	4.07	14.98	207	3.92	0.93	Daily
Min	0.09	9.79	208	4.45	0.71	Daily
Pumped water						
Mean	7.19	17.15	207	2.07	0.81	Monthly
Discharge zone						
Mean	7.85	13.24	194	2.27	0.81	Daily
Control zone						
Mean	7.23	11.21	203	1.83	0.77	Daily

## 5. Adaptation trends

Water temperatures were measured along transects parallel to flow during the time period 1997–2002, providing interior surface  $T$  data at five distances on twenty dates. However, only ten of those occasions had conditions of reasonably large (ca 2–5 °C) temperature changes as well as flowing water from the pump. During some months, the temperature gradient from inlet to outlet was too small to allow parameter estimation for  $\eta$ . Fig. 3 provides examples of the data fit using the accommodation coefficient. The adaptation of the warm incoming water to wetland energy balance conditions was rapid. The change over process from inlet  $T$  to balance  $T$  is termed accommodation. Surface water transect temperature data show that the accommodation is complete in about 100 m from the discharge (Fig. 3). This corresponds to a nominal water travel time of about 2 days, based on the average flow to the wetland at that time. However, the local water velocity at the transect locations could have been somewhat different, and measurement of the local velocity was not possible. More information on water depths and flows is found in Kadlec (2009a).

The value of the accommodation time is  $\tau_A = 0.48$  d, and the accommodation coefficient  $\eta = 1.76$  MJ/m<sup>2</sup> d °C for this data from early in the project (1978). At that time, the accommodation region was vegetated by sedges (*Carex* spp.), which were replaced by cattails (*Typha latifolia*) after a few years (Kadlec, 2009c). It is therefore not surprising that this accommodation coefficient is different from those subsequently measured in the cattail cover type. A further complicating factor was the development of a floating mat in the immediate area of the discharge (Kadlec, 2009b).

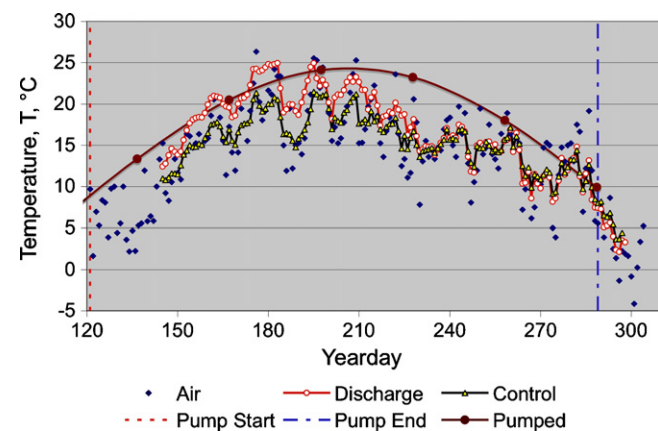


**Fig. 2.** Progression of mean daily air and water temperatures in 1997. The discharge and control sites were above the litter surface. The pumped water temperatures have been indicated with a sinusoid, for clarity.

The transect probe measurements of surface temperature were regressed to Eq. (2), and resulted in  $\eta = 1.18 \pm 0.56$  MJ/m<sup>2</sup> d °C. The corresponding values of the accommodation time were  $\tau_A = 0.87 \pm 0.39$  d. These regression values must be regarded as estimates, because most of the temperature drop occurred over the first two or three sampling distances.

The balance temperatures ( $T^*$ ) for the wetland may be determined in two ways from the project temperature data. First, the surface water temperatures in zones outside the adaptation region may be regarded as balance temperatures, because they reflect no influence of the incoming water. On any given date, these may be averaged to form an estimate of the regional wetland balance temperature. Additionally, transect data may be fit with the model Eq. (2), and the downstream plateau temperature thus determined represents the balance temperature on the date of that transect (Fig. 3). Second, the vertical soil temperature profiles contain the surface temperature as the upper extreme. The probe data on any given date has large variability in surface temperature, because of diurnal cycles and local spatial variability. However, the lower soil horizons provide a strong integrative effect, and smooth short-term variability. Thus the Eq. (5) model values may be regarded as the long-term stable equilibrium temperatures. In particular, the calibrated model temperature cycle at the soil surface was a good estimator for the wetland balance temperatures in the surface water. This estimate utilizes temperatures at a variety of depths to support a model of

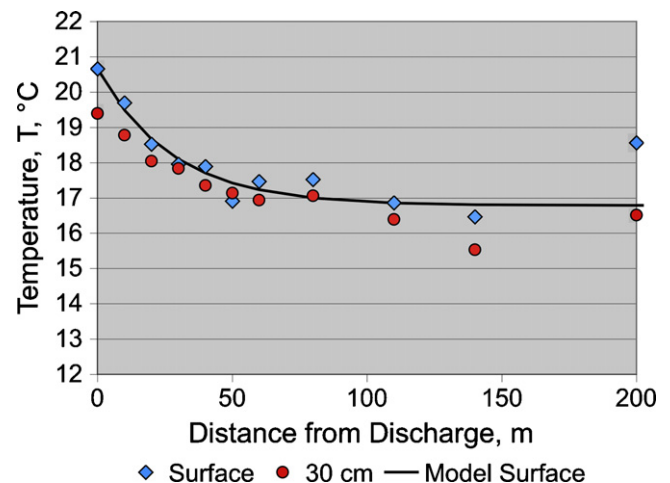


**Fig. 3.** Exponential fit to transect data for surface water temperature on 8/30/78. The plateau, or balance temperature is 16.8 °C. The value of  $R^2 = 0.95$ . Corresponding data from a depth of 30 cm into the soil is shown for reference. The average water velocity was approximately 60 m/d, but may have differed somewhat at this transect. The value of the accommodation time is  $\tau_A = 0.48$  d, and the accommodation coefficient  $\eta = 1.76$  MJ/m<sup>2</sup> d °C.

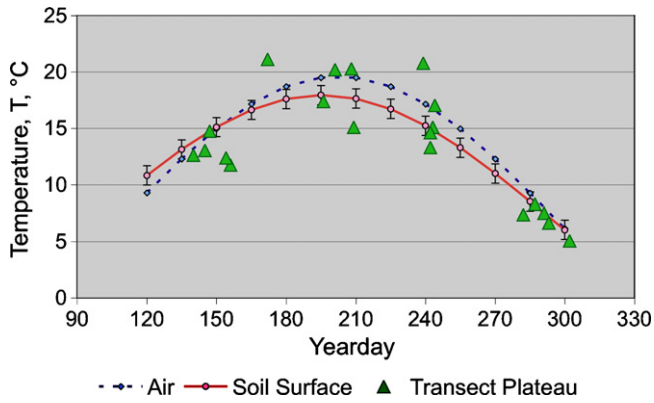


**Fig. 4.** Balance water temperatures for the Houghton Lake wetland estimated from soil surface and transect plateau methods. Soil surface  $T$  estimates are from Eq. (5), calibrated to several other deeper depths. Error bars on the soil surface represent the standard deviation among data fits at multiple locations.

surface temperature cycles, as discussed in more detail in the next section.

There was close agreement among various stations for the calibrated surface temperature model (Fig. 4), with a standard deviation of less than one degree. The values of the balance temperature for surface water transects display a much larger scatter, but are distributed around the surface cycle curve. Balance water temperatures are generally a degree or two lower than the mean daily air temperature.

**6. Soil temperatures**

The cycle in surface water temperature causes cycles in the underlying soil strata, which are delayed in time because of the thermal inertia of the soil column. That same thermal inertia provides a buffer against the diurnal variations of surface temperatures, providing strong suppression of those large variations. At just 30 cm down in the soil, the mean daily swing in warm season temperatures was only about 1 °C (Table 1). The annual cycles, and the accompanying vertical temperature profiles, are of considerably more interest, because these control the flow of heat to and from the root zone over the course of the year.

Soil temperatures at the 30 cm horizon, in both control and discharge locations, were logged during the irrigation season of 1997 (Fig. 5). The placement of the control logger was at 45 cm, but the

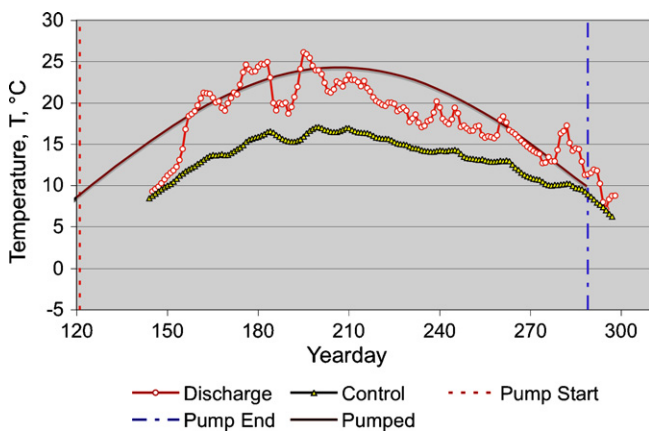


**Fig. 5.** Progression of mean daily soil temperatures in 1997. The discharge and control sites were 30 cm below the soil surface. The pumped water temperatures have been fit with a sinusoid, for clarity.

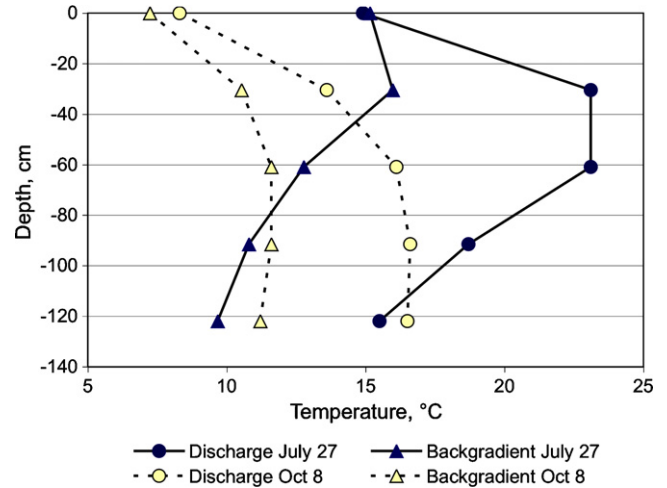


**Fig. 6.** Vertical temperature profiles in 2001. Pumped water temperatures were 24.0 °C in July and 12.2 °C in October. Mean daily air temperatures were 12.8 °C on July 27 and 1.1 °C on October 8.

temperatures were corrected to 30 cm using the depth regressions of the probe measurements. The average correction was +1.6 °C. The soil temperature at the discharge location was at an average of 4.7 °C warmer than at the control location, and the maximum difference was 10.2 °C. Throughout much of the irrigation season, the discharge area soil temperature was near the pumped water temperature. This is likely attributable to the presence of the floating mat, because the 30 cm horizon was at approximately the bottom of the mat, and hence in close proximity to the under-mat flowing water. Temperatures at the discharge site were more variable than at the control site, and showed some indications of responding to rainfall and pump shut-off events.

The thermal consequences of under-mat flow are further illustrated by the presence of a maximum in the vertical profile at the 30–60 cm horizon (Fig. 6). In midsummer, warmer temperatures prevail at this depth in the discharge zone, by about 10 °C. Warm pumped water was under-flowing the cooler mat. This difference shrank to about 4 °C at the end of the pumping season.

During the summer months, heat is transferred down into the soil in response to a negative downward gradient in soil temperature (Fig. 7). During winter, that stored heat energy is transferred back upward, and counteracts to some degree the cooling effect of the cold winter air. Because the annual cycle is largely repetitive, the amounts of gained and lost soil energy are virtually identical

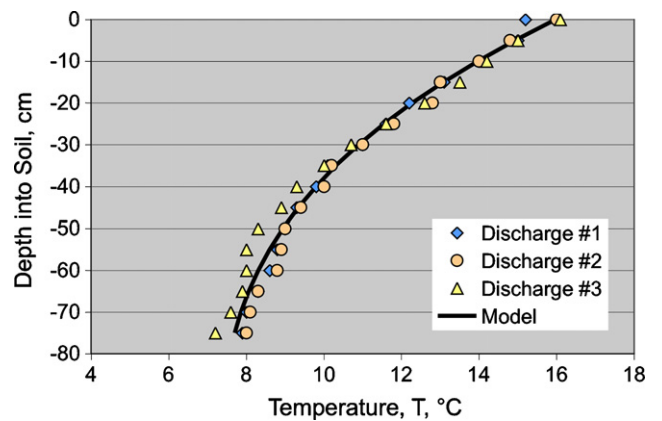


**Fig. 7.** Temperature variation with depth on June 1, 1979, at three discharge locations. The line represents the model of Eq. (5).

**Table 3**  
Soil temperature model parameters. There were six background stations and one discharge station, monitored for 6 years 1997–2002. Stations in 1978–1979 were regarded as “background” if further than 100 m from the discharge. Measurements were at four to six depths, at 30 cm intervals. See Fig. 2 for an example of the fit. The top two horizons, 30 and 60 cm, were not used in the discharge 1997–2002 data fitting, because the model was invalid in that region.

Parameter	Units	Background		Discharge	
		1978–1979	1997–2002	1978–1979	1997–2002
$T_{\text{mean}}$	°C	9.01	7.93 ± 0.42	7.11	11.4
$A$	–	1.66	1.30 ± 0.14	1.72	1.96
Surface Amplitude	°C	14.97	10.26 ± 0.69	12.26	22.4
$t_{\text{max}}$	Yearday	184	196 ± 6	205	154
$\alpha$	m <sup>2</sup> /d	0.0045	0.0085 ± 0.0019	0.0162	0.0048
$H$	m	0.73	0.99 ± 0.12	1.37	0.74
$R^2$		0.99	0.84 ± 0.05	0.94	0.73
Yearday of max flux		321	333 ± 6	341	333
Maximum flux	MJ/m <sup>2</sup> d	1.51	0.77 ± 0.11	0.65	2.2
Half cycle gain/loss	MJ/m <sup>2</sup>	175	90 ± 13	76	256
Half cycle flux	MJ/m <sup>2</sup> d	0.96	0.49 ± 0.07	0.42	1.40

in magnitude. Detailed vertical temperature profiles, in conjunction with soil properties, allow the calculation of vertical energy flows. Data such as that shown in Fig. 7 are often quite regular, and is well described by Eq. (5). The fit of that example triplicated vertical profile has an  $R^2 = 0.997$  when parameterized by  $T_s$ ,  $A$  and  $H$ .

More complete datasets include vertical profiles determined at several times during the year. The fitting of the set of profiles then additionally requires determination of the time of the surface temperature maximum,  $t_{\text{max}}$ . Various heat fluxes may then be computed through use of Eqs. (6)–(9).

Two sets of vertical profiles were acquired, in 1978–1979 and in 1997–2002. The earlier set was for a nearly unaltered wetland, with no cattails and no floating mat. The later set was for a highly altered wetland, with cattails dominant and a floating mat near the discharge (Kadlec, 2009c). The values of ( $T_s$ ,  $A$ ,  $H$  and  $t_{\text{max}}$ ) were selected to minimize the error between data and model for each of the two periods of study. Because of the high variability of surface water temperatures, these were not included in the error minimization, but the predicted time series was produced nonetheless. The resulting parameter values are shown in Table 3. Standard deviations were computed only for the six background stations in the second period, because the sampling protocol had only one station near the discharge at most times. An example of the goodness of fit is shown in Fig. 8.

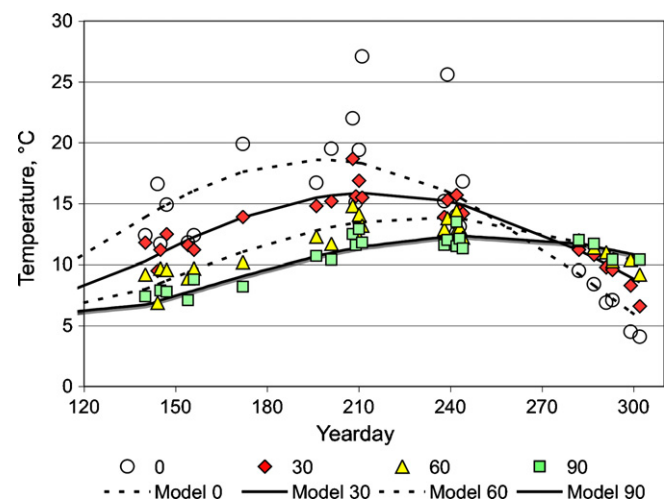


**Fig. 8.** Soil temperatures in a background control zone of the wetland, 500 m from the discharge. Data were taken monthly over a 6-year period, 1997–2002. Model fit parameters are  $T_s = 8.05$  °C,  $A = 1.31$ ,  $H = 1.02$  m and  $t_{\text{max}} = 197$  d. The  $R^2 = 0.90$ .

### 7. Discussion and conclusions

The water temperature in treatment wetlands is of interest for several reasons, prominently including the fact that water temperature modifies the rates of several key biological processes. There is extensive literature supporting the strong effect of temperature on microbial nitrogen processing, with doubling of nitrification and denitrification rates over a temperature range of about 10 °C (Kadlec and Wallace, 2008). Therefore, knowledge of wetland water temperature is a necessary prerequisite in wetland design.

The water entering the wetland was typically somewhat warmer than the background wetland conditions. That extra warmth was capable of enhancing microbial processes, including those that result in gas generation, such as respiration, methanogenesis and denitrification. Speculatively, this enhanced gas generation may have contributed to the formation of the floating mat, by increasing the buoyancy of the root zone.

Clearly it matters what time of day is used to measure water temperatures. For example, the magnitude of the water temperature variation was in the range of 3–20 °C (median 10 °C, Table 1), large enough to support a doubling of the rate coefficient for denitrification, during a 24-h cycle. Because maximum and minimum daily values occurred at the two ends of the working day, the timing of data collection is critical. Indeed, the magnitude of the seasonal water  $T$  cycle is not much greater than the magnitude of the daily cycle. Because of the ready availability of inexpensive  $T$  loggers, it is advisable to avoid synoptic measurements during the course of the day.

There are two regional aspects of wetland water temperature status: the adaptation zone and the balance zone. Water to be treated typically enters the wetland at a temperature different from the balance temperature, and changes to the balance temperature as the water progresses through the adaptation zone of system. That alteration generally follows an exponential curve, and the distance for accommodation may be estimated from knowledge of the accommodation coefficient ( $\eta$ ). Use of this coefficient relies upon the hydraulic loading in the adaptation zone. The alternative approach is use of the accommodation time constant ( $\tau_A$ ), which relies upon the time of travel and the depth of water. Because there is frequently a good deal of uncertainty about water depth, the accommodation coefficient alternative is to be preferred. The range of accommodation coefficients for a number of warm-climate wetlands was reported as 0.27–2.50 MJ/m<sup>2</sup> d °C (Kadlec and Wallace, 2008). This brackets the values of 1.18 and 1.76 MJ/m<sup>2</sup> d °C determined for the early and late periods of the Houghton Lake wetland record. The range of corresponding time constants was reported as 0.78–3.70 d (Kadlec and Wallace, 2008). The values of 0.48 and 0.87 d were determined for the early and late periods of the

Houghton Lake wetland record, which are at the low end of the warm wetland range. The reason for this is that water depths at Houghton Lake were much lower than for the literature systems (10–20 cm at Houghton Lake; 45–60 cm for literature systems).

The balance temperatures represent the limit reached after passage through the adaptation zone. Direct measures of surface water temperatures in that zone were found to possess considerable scatter, even if loggers were used. It was found that scatter could be removed by utilizing soil temperature data as a function of depth and time to estimate the surface temperature. The soil energy storage capacity integrates and smoothes the variations, and provided a representation of the central tendency of the stochastic direct measurements of water temperature.

The balance temperatures may also be estimated from an energy balance on the water and vegetation, as documented in Kadlec and Knight (1996). That procedure requires quite a lot of meteorological data, including incident radiation, wetland reflectance, sunshine fraction, relative humidity, and wind speed (Scheffe, 1978). The resulting effects on wetland water temperature are important. For example, incoming water in an arid climate treatment wetland in Arizona was found to cool considerably upon passage, to well below the ambient air temperature, due to evaporative cooling (Kadlec, 2006). However, the Houghton Lake climate was cooler ( $10 < T < 20^{\circ}\text{C}$ ) and moister (relative humidity ca. 70%). The energy balance procedure forecasts that under these conditions, the wetland water balance temperatures should be close to the mean daily air temperatures (Kadlec and Wallace, 2008). This was indeed the case (Fig. 2).

Forecasts of balance temperatures for other treatment wetlands may therefore require such an energy balance calculation. In the event of very wet or very dry climates, the water (and surface soil) balance temperatures will deviate from the mean daily air temperature as documented in Kadlec and Wallace (2008). A further consequence is that the vegetative canopy will influence the water temperature, as shown in Kadlec (2006). For the driving boundary condition of surface temperature, the two parameters are the amplitude of the cycle and the time of the annual maximum. There is very little intra-system variability in the expected date of the annual maximum; it is about 3 weeks after the summer solstice (Kadlec and Wallace, 2008). The boundary condition of surface temperature is therefore determined almost exclusively by the amplitude of the surface temperature cycle. Nonetheless, the surface temperatures remain sinusoidal, and the analysis in this paper still applies to below-ground temperatures in the balance zone.

The larger data gap for extrapolation to other wetlands is the lack of information on the thermal diffusivity ( $\alpha$ ) for the top soil layers of the wetland. Penetration depths are a meter or two, and are likely to be water saturated. Ideally, it would be useful to have data for the thermal diffusivity, or the contributing thermal conductivity, density and heat capacity—see Eq. (7). Unfortunately, such data is not commonly available for under-wetland soils, which is why a data fitting process was used here.

There are three potential regimes for vertical temperature profiles in the water column that have been observed in wetlands and shallow ponds. There may be no vertical profile at all, a condition of no thermal stratification. The second situation is no vertical profile during the night, but the development of surface heating during the daytime hours. This is termed diurnal mixing. The third case is the existence of a vertical temperature gradient throughout the entire 24-h period, called stratification. Condie and Webster (2001) present a criterion for stratification, which is reproduced in Kadlec and Wallace (2008). For conditions in the Houghton Lake wetland, no stratification was to be expected, and anecdotal data indicated none. This result is consistent with the more extensive studies of Chimney et al. (2006). The water column could therefore be consid-

**Table 4**

Ranges of energy flows for summer and winter conditions. The winter heat losses to the air are predicated on a range of temperature differentials of  $-5^{\circ}\text{C}$  to  $-15^{\circ}\text{C}$ , and a range of thermal resistances due to snow, litter and ice of  $10\text{--}40\text{ (MJ/m}^2\text{ d }^{\circ}\text{C)}^{-1}$ . In winter, heat is lost to air, and gained from the deep soils. Refer to Kadlec and Knight (1996) and Kadlec and Wallace (2008) for details.

Energy flux		Summer	Winter
<b>Inputs</b>			
Undepleted solar radiation <sup>a</sup>	MJ/m <sup>2</sup> d	30–40	–
Ground surface solar input <sup>b</sup>	MJ/m <sup>2</sup> d	16–22	–
Reflected radiation <sup>c</sup>	%	15–30	–
Back radiation (heat) <sup>d</sup>	MJ/m <sup>2</sup> d	4–5	–
Net incoming radiation	MJ/m <sup>2</sup> d	8–12	–
Convective energy from air <sup>e</sup>	MJ/m <sup>2</sup> d	0.1–0.5	–(0.1–1.5)
<b>Outputs</b>			
Evapotranspiration <sup>f</sup>	mm/d	2.5–3.5	–
ET heat loss	MJ/m <sup>2</sup> d	7–10	–
Soil heat recharge <sup>g</sup>	MJ/m <sup>2</sup> d	0.4–1.4	–(0.4–1.4)

<sup>a</sup> From solar tables, for the latitude and season.

<sup>b</sup> After deductions for cloud cover and absorption by carbon dioxide and water.

<sup>c</sup> Estimated from literature wetland data.

<sup>d</sup> Calculated from the Stefan-Boltzman formula.

<sup>e</sup> Calculated from wind speed and air and surface temperatures.

<sup>f</sup> Estimated from pan data.

<sup>g</sup> Calculated from methods in this paper.

ered vertically uniform, but changes in energy storage in the water may nonetheless be important (Shoemaker et al., 2005).

The temperature variation in the root zone (30 cm) is muted considerably compared to surface water temperature cycles (see Fig. 5). While the mean temperature during the operating season was  $1.3^{\circ}\text{C}$  lower at 30 cm, the swings were only  $3.6^{\circ}\text{C}$  at 30 cm, compared to  $6.4^{\circ}\text{C}$  at the surface.

Below-surface temperatures are of interest for several reasons. As discussed above, these provide a means of estimating the water balance temperature. Further, microbial processes in the root zone are modulated by root zone temperature. In a situation of undermat flow, regular cyclic concepts no longer apply, but subsurface temperature is now the determinant for biological processes in the flowing water. For extended periods of operation to cold seasons, a knowledge of soil temperatures is essential to estimating the upward cold season heat fluxes that counter the loss of energy to the cold air above. Soil heat fluxes are small in comparison to incoming radiation and evaporative heat loss in summer months, but not in winter (Table 4). In summer, radiation is the dominant input and ET loss is the dominant output. These are both small or absent in winter, due to a snow and ice cover. However, winter heat loss through the snow, litter and ice cover to the cold air above is the dominant loss factor, while heat gain from the deep soils is the only gain factor. The numbers in Table 4 suggest that under some conditions (e.g., thick snow blanket), soil heat will be greater than heat loss to the air. The implication is a prevention of freezing under the snow, and that situation was observed at the Houghton Lake site. Conversely, in the absence of an insulating snow layer, heat loss to the air caused ice formation—to typical thicknesses of 20 cm. Thus soil heat release is a critical factor in the operability of a wetland under cold conditions. The values of the soil heat return fluxes from the soil model are shown in Table 3. For further elucidation of the summer energy balance, the reader is referred to Kadlec and Knight (1996). For further elucidation of the winter energy balance, the reader is referred to Kadlec and Wallace (2008).

The choice of level of detail in a quantitative model of the near-surface energy transfer processes spans a considerable range of complexity. The most detail, and the most intuitively satisfying choice combines energy balances for the canopy, water layer and the soil layers below (Hares and Novak, 1992; Ji, 1995; Zhang et

al., 2002). However, such mechanistic models contain numerous process parameters, and demand a large amount of meteorological data as input. And, these are rarely spatially distributed to account for the presence of flowing water. The four parameters of the spatial-temporal model of Eqs. (2) and (5) are easier to use, and appear to contain sufficient detail.

Gonzalez-Rouco et al. (2003) tested terrestrial deep soil temperature (TDST) as a proxy for surface temperature (SAT). In the simulation, at interannual time scales, the connection between TDST and SAT was stable, but stronger in the summer half-year than in the winter half-year. At long timescales, annual TDST was a good proxy for annual surface temperature, and their variations were almost indistinguishable from each other. Their suggestion has been followed in this analysis of the Houghton Lake treatment wetland, and found to be a useful way to reduce variability.

It is concluded that the thermal condition of this treatment wetland was quantifiable via commonly accepted models, with parameters that were within the range of other similar system studies. However, the adaptation zone was more complicated, due to the presence of a floating mat and water under-flow. This altered thermal regime should be accounted in detailed design and forecasting procedures.

## References

- Boone, R.D., Nadelhoffer, K.J., Canary, J.D., Kaye, J.P., 1998. Roots exert a strong influence on the temperature sensitivity of soil respiration. *Nature* 396, 570–572.
- Chimney, M.J., Wenkert, L., Pietro, K.C., 2006. Patterns of vertical stratification in a subtropical constructed wetland in south Florida (USA). *Ecol. Eng.* 27 (4), 322–330.
- Condie, S.A., Webster, I.T., 2001. Estimating stratification in shallow water bodies from mean meteorological conditions. *J. Hydraul. Eng.* 127 (4), 286–292.
- Gonzalez-Rouco, F., von Storch, H., Zorita, E., 2003. Deep soil temperature as proxy for surface air-temperature in a coupled model simulation of the last thousand years. *Geophys. Res. Lett.* 30 (21) (art. 2116).
- Hares, M.A., Novak, M.D., 1992. Simulation of surface energy balance and soil temperature under strip tillage. I. Model description. *Soil Sci. Soc. Am. J.* 56, 22–29.
- Ji, J., 1995. A climate vegetation interaction model: simulating physical and biological processes at the surface. *J. Biogeogr.* 22, 445–451.
- Kadlec, R.H., Knight, R.L., 1996. *Treatment Wetlands*. CRC Press, Boca Raton, FL, pp. 893.
- Kadlec, R.H., 1999. Chemical, physical and biological cycles in treatment wetlands. *Water Sci. Technol.* 40 (3), 37–44.
- Kadlec, R.H., 2001. Thermal environments of subsurface treatment wetlands. *Water Sci. Technol.* 44 (11/12), 251–258.
- Kadlec, R.H., 2006. Water temperature and evapotranspiration in surface flow wetlands in hot arid climate. *Ecol. Eng.* 26 (4), 328–340.
- Kadlec, R.H., Wallace, S.D., 2008. *Treatment Wetlands*, second ed. CRC Press, Boca Raton, FL.
- Kadlec, R.H., 2009a. Wastewater treatment at Houghton Lake, Michigan: hydrology and water quality. *Ecol. Eng.* 35 (9), 1287–1311.
- Kadlec, R.H., 2009b. Wastewater treatment at the Houghton Lake wetland: soils and sediments. *Ecol. Eng.* 35 (9), 1333–1348.
- Kadlec, R.H., 2009c. Wastewater treatment at the Houghton Lake wetland: vegetation response. *Ecol. Eng.* 35 (9), 1312–1332.
- Mihalakakou, G., Santamouris, M., Lewis, J.O., Asimakopoulos, D.N., 1997. On the application of the energy balance equation to predict ground temperature profiles. *Solar Energy* 60 (3–4), 181–190.
- Priban, K., Jenik, J., Ondok, J.P., Popela, P., 1992. Analysis and modeling of wetland microclimate. In: *Studie CSAV 2-92*. Academia, Prague.
- Scheffe, R.D., 1978. Estimation and prediction of summer evapotranspiration from a Northern Wetland, MS Thesis, University of Michigan, Ann Arbor, MI.
- Seabloom, E.W., van der Valk, A.G., Moloney, K.A., 1998. The role of water depth and soil temperature in determining initial composition of prairie wetland coenoclines. *Vegetatio* 138 (2), 203–216.
- Shoemaker, W.B., Sumner, D.M., Castillo, A., 2005. Estimating changes in heat energy stored within a column of wetland surface water and factors controlling their importance in the surface energy budget. *Water Resour. Res.* 41 (W10411), 18.
- Zhang, Y., Li, C., Trettin, C.C., Li, H., Sun, G., 2002. An integrated model of soil, hydrology, and vegetation for carbon dynamics in wetland ecosystems. *Global Biogeochem. Cycles* 16 (4) (art. 1061).